Cell. Mol. Life Sci. (2010) 67:4213–4232
DOI 10.1007/s00018-010-0431-6

Cellular and Molecular Life Sciences

RESEARCH ARTICLE

ADAMTS-2 functions as anti-angiogenic and anti-tumoral molecule independently of its catalytic activity

J. Dubail · F. Kesteloot · C. Deroanne · P. Motte · V. Lambert · J.-M. Rakic · C. Lapière · B. Nusgens · A. Colige

Received: 14 January 2010 / Revised: 26 May 2010 / Accepted: 2 June 2010 / Published online: 24 June 2010

Abstract ADAMTS-2 is a metalloproteinase that plays a key role in the processing of fibrillar procollagen precursors into mature collagen molecules by excising the aminopropeptide. We demonstrate that recombinant ADAMTS-2 is also able to reduce proliferation of endothelial cells, and to induce their retraction and detachment from the substrate resulting in apoptosis. Dephosphorylation of Erk1/2 and MLC largely precedes the ADAMTS-2 induced morphological alterations. In 3-D culture models, ADAMTS-2 strongly reduced branching of capillary-like structures formed by endothelial cells and their long-term maintenance and inhibited vessels formation in embryoid bodies (EB). Growth and vascularization of tumors formed in nude mice by HEK 293-EBNA cells expressing ADAMTS-2 were drastically reduced. A similar anti-tumoral activity was observed when using cells expressing recombinant deleted forms of ADAMTS-2, including catalytically inactive enzyme. Nucleolin, a nuclear protein also found to be associated with the cell membrane, was identified as a potential receptor mediating the antiangiogenic properties of ADAMTS-2.

Keywords ADAMTS · Angiogenesis · Cell adhesion · Apoptosis · Tumor

Abbreviations

EB	Embryoid body
EBM	Endothelial basal medium
ES cell	Embryonic stem cell
HEK 293-EBNA cell	Human embryonic kidney 293-Epstein Barr nuclear antigen cell
HMEC	Human microvascular endothelial cell
HMVEC	Human dermal microvascular endothelial cell
HSF	Human skin fibroblasts
HSMC	Human smooth muscle cell
HSPG:	Heparan sulfate proteoglycan
HUVEC	Human umbilical vein endothelial cell
MLC	Myosin light chain
mTS2	Catalytically inactive ADAMTS-2
PAK	p21 Activated kinase
PECAM	Platelet endothelial cell adhesion molecule: CD31
ROCK	Rho kinase
TSR1	Thrombospondin repeat type 1

Electronic supplementary material The online version of this article (doi:10.1007/s00018-010-0431-6) contains supplementary material, which is available to authorized users.

J. Dubail · F. Kesteloot · C. Deroanne · C. Lapière · B. Nusgens · A. Colige (✉)
Laboratory of Connective Tissues Biology, GIGA-R, Tour de Pathologie, B23/3, 4000 Sart Tilman, Belgium
e-mail: acolige@ulg.ac.be

P. Motte
Laboratory of Plant Cellular Biology, Sart Tilman, Belgium

V. Lambert
Laboratory of Development and Tumor Biology, University of Liège, Sart Tilman, Belgium

J.-M. Rakic
Department of Ophthalmology, University Hospital, Sart Tilman, Belgium

TS-2	ADAMTS-2
wtTS2	Wild-type ADAMTS-2

Introduction

Angiogenesis, the process by which neovasculature is formed from existing blood vessels, is essential in normal development and plays a critical role in several pathological conditions such as cancer, rheumatoid arthritis, and diabetic retinopathy [1, 2]. Vascularization of tumors is critical for their growth beyond a few mm^3 [3] and for cancer cells to escape to distant sites through hematogenous spreading and metastasis. Accordingly, it was proposed that inhibition of angiogenesis could be an efficient anti-cancer therapy that further targets genetically stable cells [3]. In this context, identification and characterization of endogenous inhibitors of blood vessel formation is of critical importance. It is anticipated that they should be less prone to induce side-effects and resistance to treatment than synthetic inhibitors.

In recent years, a number of endogenous inhibitors of angiogenesis have been identified, many of them deriving from extracellular matrix (ECM) components. Some of these inhibitors are effective either as native full-length proteins or as proteolytic fragments [2]. This is the case for thrombospondins (TSP) 1 and 2, for which the mechanisms leading to inhibition of angiogenesis have been extensively studied and characterized [4]. Short sequences present in the N-terminal domain, especially in the thrombospondin type 1 repeats (TSR1), are released by ADAMTS-1 [5] and inhibit angiogenesis by interacting with the CD36 scavenger receptor [6–8]. Another class of inhibitors are active only as fragments derived from larger matrix macromolecules such as type XVIII collagen (endostatin), type XV collagen (restin), the α1, α2, and α3 chains of type IV collagen (arresten, canstatin, and tumstatin) and perlecan (endorepellin) [1]. Signaling from these molecules most probably involves binding or interference with specific integrins [1, 9]. A third class of angiogenesis regulators comprises secreted enzymes, most of which are pro-angiogenic by facilitating endothelial cells migration through degradation of matrix macromolecules and promoting the release of pro-angiogenic cytokines and growth factors immobilized in the ECM. However, some of these enzymes can also, in defined circumstances, inhibit angiogenesis. Angiostatin, a potent inhibitor of angiogenesis, is a proteolytic fragment of plasminogen [10, 11] and matrix metalloproteinases can generate anti-angiogenic fragments by proteolytic processing of some ECM proteins (see above, and [12]). As another example, two metalloproteinases of the ADAMTS family, ADAMTS-1 and -8, were also reported to strongly inhibit angiogenesis [13, 14]. The most striking characteristic of the ADAMTS enzymes is the presence, in addition to the metalloproteinase and disintegrin domains, of at least one domain highly similar to the TSR1 found in thrombospondins 1 and 2. Studies investigating the anti-angiogenic properties of ADAMTS-1 suggest that several domains are implicated, including a TSR1 domain [15]. The catalytic activity of ADAMTS-1 is also implicated in its anti-angiogenic function since it alters in vitro endothelial cells adhesion and migration [15] and is essential for inhibiting angiogenesis in vivo in xenograft assays [16]. It may also act by interacting with VEGF [13].

Among the other members of the ADAMTS family, ADAMTS-2 is one of the best characterized [17, 18]. It contains four TSR1 domains and a RGD sequence in a Cys-rich domain that could potentially bind to integrins. Its primary function is to cleave the amino propeptides of type I, II, III and V procollagens [19–21], explaining its previous name “aminoprocollagen peptidase”. Mutations in the ADAMTS-2 gene cause dermatosparaxis in human (dermatosparactic type of Ehlers-Danlos syndrome, also known as Ehlers-Danlos syndrome type VIIC) and other mammals [20, 22]. This inherited connective tissue disorder arises as a result of accumulation of incorrectly processed aminoprocollagen and its cardinal feature is an extreme skin fragility. *Adamts2* knockout mice have been created [23]. In addition to skin fragility, male infertility was related to altered maturation of spermatogonia, suggesting that ADAMTS-2 may have functions other than procollagen processing. An alternative splicing mechanism and complex maturation processes of the secreted enzyme have been described, generating various polypeptides that are not implicated in procollagen processing [19].

In this work, the anti-angiogenic properties of ADAMTS-2 in vitro and in vivo are demonstrated and initial characterizations of the mechanisms involved in its biological activity are reported.

Materials and methods

Cell cultures

Human umbilical vein endothelial cells (HUVEC) were isolated as previously described [24]. Human dermal microvascular endothelial cells (HMVEC) were purchased from LONZA (LONZA, Verviers, Belgium). HUVEC and HMVEC were seeded on gelatin-coated culture dishes and grown in endothelial basal medium (EBM) supplemented with SingleQuot® Kit (LONZA). Human microvascular endothelial cells (HMEC) [25], human primary skin

fibroblasts (HSF) [26], and human smooth muscle cells (HSMC) [27] were grown in Dulbecco's modified Eagle's medium (DMEM, Invitrogen, Grand Island, NY) supplemented with 10% FBS (LONZA). Heparinase III and chondroitinase were purchased from Sigma (Sigma-Aldrich, St. Louis, MO, USA).

Production and purification of wild recombinant ADAMTS-2 and controls

Recombinant bovine ADAMTS-2 was produced in HEK 293-EBNA cells as previously described [19]. Although recombinant ADAMTS-2 was highly purified [19], co-purification of any product secreted by HEK 293-EBNA cells that could potentially hamper the analysis of experimental data could not be totally excluded. In order to take into account this possibility, control samples were produced from HEK 293-EBNA cells transfected with the empty vector using the same purification procedures as described for recombinant ADAMTS-2. The electrophoretic patterns of purified control medium and of purified ADAMTS-2 was determined on a SDS-PAGE stained with SYPRO® Ruby Protein Gel Stain (BioRad, Hercules, CA) as described by the manufacturer. For any experimental condition, the effect of ADAMTS-2 was always compared to the effect observed with a similar volume of the purified control medium.

Cell proliferation assay

Cell proliferation assays were performed by two different methods. In the first one, cells were seeded (HMEC: 2.5×10^4 cells/cm^2; HUVEC, HMVEC, HSF: 1×10^4 cells/cm^2) in 24-multiwell plates (Cellstar, Greiner Bio-one Frickenhausen, Germany) coated with gelatin in EBM supplemented with 0.5% FBS. After 3 h, the medium was discarded and cells were incubated in EBM containing 0.5% FBS and ADAMTS-2 or the control sample. After 24 h, the culture medium was replaced by the same medium containing 0.4 µM [^{3}H]-thymidine (6.7 Ci/mmol; PerkinElmer Life Sciences, Boston, MA, USA) and 0.6 µM cold thymidine (Sigma-Aldrich). After 20 h, cells were washed twice with DMEM and sonicated in 500 µl PBS. Incorporation of thymidine was determined by measuring the TCA (cold, 5% final) insoluble radioactivity collected by filtration on glass microfiber filters (GF/A, Whatmann, Maidstone, United Kingdom).

For the second method, HEK 293-EBNA cells were seeded (1.6×10^4 cells/cm^2) in 6-multiwell plates (Cellstar) in DMEM supplemented with 10% FBS. At days 0, 1, 2, 3, 4 and 5, the DNA was measured by a fluorimetric technique using bis-benzimide [28].

Cell morphology and immunocytochemical staining

In a first set of experiments, cells were seeded on gelatin-coated 24-multiwell plates in EBM supplemented with 0.5% FBS. In a second set of experiments, cells were seeded in non-supplemented EBM on gelatin-coated or fibronectin-coated (0.25 µg/cm^2) 4-wells LabTek© chambered coverglasses (Nalge Nunc International, IL, USA) for immunocytochemical staining or on gelatin-coated or fibronectin-coated 24-multiwell plates for observation by phase contrast microscopy. For all experiments, the medium was discarded after 3 h of attachment and spreading, and replaced by fresh medium containing, when indicated, 5 µg/ml of ADAMTS-2 or control sample. After 16 h, cells were fixed with 3% formaldehyde in PBS for 30 min and permeabilized for 3 min in PBS containing 0.1% Triton® X-100 (Merck, Darmstadt, Germany). Vinculin staining was performed using a monoclonal antibody against vinculin (dilution 1:1,000 for 1 h; V9131; Sigma-Aldrich) followed by Alexa Fluor 546 rabbit anti-mouse IgG (2 µg/ml final concentration, for 1 h; Molecular Probes, Eugene, OR, USA), F-actin was stained with 100 ng/ml FITC-Phalloidin (Sigma-Aldrich) in PBS for 20 min. Nuclei were stained with 0.2 µg/ml bis-benzimide (Calbiochem, La Jolla, CA, USA) in PBS. After mounting using Aqua Poly/Mount (Polysciences, INC, Warrington, PA, USA), cells were observed with Zeiss Axiovert 25 microscope equipped with an Axiocam Zeiss camera and the KS 400 Kontron image analysis software.

Time-lapse video imaging

HUVEC and HSF were seeded (3.3×10^4 cells/cm^2) in Glass Bottom Culture Dishes No. 1.5 coated with collagen (MatTek Co, Ashland, MA) in EBM supplemented with 0.5% FBS. After 5 h, the medium was replaced by fresh medium containing 5 µg/ml of ADAMTS-2 or control sample. Time-lapse videomicroscopy was performed using a Leica TS-2 confocal microscope (Leica, Wetzlar, Germany). Images were recorded every 5 min for 20 h. All time-lapse imaging was performed under 5% CO_2 and 37°C in a controlled stage incubator.

Western-blot analysis

HUVEC were seeded (3.3×10^4 cells/cm^2) on gelatin-coated 24-multiwell plates in serum-free EBM. After 3 h, ADAMTS-2 was added in the medium to obtain a final concentration of 5 µg/ml. The same volume of the control sample was used in parallel cultures. After increasing the time of incubation, the cells were lyzed in Laemmli denaturation buffer. Proteins were separated by SDS-PAGE and transferred onto a PVDF membrane (NEN Life

Science Products, Boston, MA, USA). After blocking with non-fat milk, membranes were incubated with primary antibody, washed, and then incubated with horseradish peroxidase-conjugated secondary antibodies (Dako, Carpinteria, CA, USA) at room temperature for 1 h. The blots were revealed by using an enhanced chemiluminescence assay (ECL, Amersham Biosciences Ltd, England) and X-ray film exposure. The antibody reagents used were: anti-phospho-p38 MAP Kinase (Biosource P0601, Camarillo, CA, USA); anti-phospho-p42/44 MAP Kinase (M-8159) and anti-MAP Kinase (M-5670) (Sigma-Aldrich); anti-phospho-myosin light chain (MLC) (Thr18/Ser 19; clone 12896) and anti-MLC (clone 15370) (Santa Cruz Biotechnology, Santa Cruz, CA, USA); anti-phospho-FAK (Tyr 397) (Upstate, Lake Placid, NY, USA); anti-FAK (BD Biosciences Pharmingen, San Jose, CA, USA); anti-phospho-p21 activated kinase (PAK) was a kind gift of M. E. Greenberg (Children's Hospital, Harvard Medical School, Boston, MA); anti-nucleolin (clone H250, Santa Cruz Biotechnology).

Apoptosis analysis

HUVEC were seeded (3.3×10^4 cells/cm^2) on gelatin-coated 12-multiwell plates (Cellstar) in serum-free EBM or in EBM supplemented with 0.5% FBS. After 3 h, medium was replaced by EBM containing 5 μg/ml ADAMTS-2 and supplemented or not with 0.5% FBS. After 30 min, 120 min, 240 min, or 18 h of incubation, medium was collected and cells were trypsinized, pooled with the medium, and centrifuged to collect any floating cells. Cells were then suspended in Annexin binding buffer (Annexin V-FITC Apoptosis Detection kit, Sigma) at the concentration of 1×10^5 cells/ml and incubated for 10 min with Annexin V-FITC (270 ng/ml) and propidium iodide (1.1 μg/ml). Cell analysis was performed using FACS (BD FACS Canto, BD Biosciences) and statistical significance was determined using one-way ANOVA test.

ADAMTS-2 immunostaining

HMEC were seeded in DMEM medium supplemented by 10% FBS. After 16 h, the medium was discarded and cells were incubated for 6 h at 8°C in serum-free medium containing, when indicated, 0.5 or 2 μg/ml of ADAMTS-2 or control sample, supplemented or not with heparin (10 μg/ml; Sigma-Aldrich). For other experiments, cells were first pretreated with 6 mU/ml heparinase III (4 h at 37°C) or 0.1 U/ml chondroitinase (4 h at 37°C), or with 20 mM sodium chlorate with or without 10 mM sodium sulfate (16 h at 37°C) before incubation with ADAMTS-2 or control sample. For all these experiments, cells after incubation with ADAMTS-2 were washed with DMEM and fixed with 3% paraformaldehyde at room temperature for 30 min. The washed cell layer was incubated sequentially in PBS containing 3% bovine serum albumin for 30 min, mouse monoclonal antibodies against ADAMTS-2 for 1 h (mAb23; [19]), Alexa Fluor 546 rabbit anti-mouse IgG for 1 h (Molecular Probes, A-11060), and, when indicated, rabbit polyclonal anti-human nucleolin (H250, Santa Cruz Biotechnology) and Alexa Fluor 488 goat anti-rabbit IgG for 1 h (Molecular Probes, A-11034). Nuclei staining was performed using DAPI at 1 μg/ml for 20 min (Roche, 236276). After mounting in Aqua Poly/Mount (Polysciences) cells were observed with a Zeiss Axiovert 25 inverted microscope.

Isolation and identification of ADAMTS-2-binding proteins

Antibody against ADAMTS-2 (mab23, [19]) was immobilized on a Affi-gel® HZ resin (Bio-Rad) as described by the manufacturer. Purified recombinant ADAMTS-2 was then incubated with resin in order to allow immobilization of ADAMTS-2 by binding with antibody against ADAMTS-2. Resin without ADAMTS-2 was used as control. Resins were poured in a column and equilibrated in 50 mM Tris HCl, pH 7.5, 2 mM $CaCl_2$, 0.1 M NaCl. HMEC were scraped from the dish and incubated 30 min on ice in extraction buffer (0.2% Triton X-100, pH 7.0, 100 mM *N*-ethylmaleimide, 0.2 mM phenylmethanesulfonyl fluoride, 5 mM benzamide). Cells were then centrifuged 25 min at 20,000 × *g*. Supernatant was collected, diluted in one volume of equilibration buffer containing NaCl to obtain 0.1% Triton X-100 and 0.1 M NaCl final concentration and loaded on column with immobilized ADAMTS-2 or on control resin. After extensive washing in the equilibration buffer, elution was performed (50 mM Tris HCl, pH 7.5, 2 mM $CaCl_2$, 0.5 M NaCl). Eluted fractions were dialyzed against 200 mM ammonium acetate and 0.01% sodium dodecyl sulfate, lyophilized, and resuspended in Laemmli buffer. Proteins were then separated by SDS-PAGE and stained by Coomassie Blue. The differential pattern between the control and ADAMTS-2 affinity chromatography allowed to identify potential proteins of interest. Their identification was performed after extraction from the polyacrylamide gel by micro high-performance liquid chromatography-electrospray ionization-trap (μHPLC-ESI-Trap; Esquire-Bruker Daltonics, Billerica, MA).

Capillary-like structures formation assay

The capillary-like structures assay was performed as previously described [29]. When indicated, 2 or 5 μg/ml ADAMTS-2 or control sample was added to the collagen solution and to the medium. Changes in cell morphology

and formation of capillary-like structures were evaluated by phase-contrast microscopy. The mean length of the structures and the number of branching per mm^2 were determined.

Embryoid bodies

Undifferentiated embryonic stem CGR8 (ES) cells were aggregated by culture on bacteriological dishes during 4 days in a 20-µl hanging drop of DMEM supplemented with 10% FBS, 0.1 mM non-essential amino acids, 0.1 mM β-mercaptoethanol, and 10 ng/ml of VEGF to induce cell clustering and differentiation into endothelial cells [30]. The aggregates were seeded on gelatin-coated glass coverslips in the same medium supplemented with recombinant ADAMTS-2 or control sample. Media were renewed every 48 h for 8 days. For immunohistochemistry, the embryoid bodies were fixed in methanol and incubated with rat anti-mouse CD31 antibodies (Pharmingen, San Diego, CA), biotin-conjugated anti-rat IgG, and streptavidin/FITC. Nuclei were stained with 0.2 µg/ml bisbenzimide (Calbiochem) in PBS. The surface of the embryoid body and the total vessel length by representative microscope field was determined by manual measurement on enlarged pictures.

Growth of HEK 293-EBNA tumors in nude mice

HEK 293-EBNA cells transfected with ADAMTS-2 cDNA (wild-type, mutated, or truncated) or empty vector [19] were resuspended at 4°C in growth factor-depleted Matrigel (BD Biosciences) solubilized in serum-free DMEM to a final concentration of 2×10^7 cells/ml. Cell suspension (100 µl) was injected subcutaneously into the flanks of mice, each mouse being injected with HEK 293-EBNA cells transfected with ADAMTS-2 on the left side and with HEK 293-EBNA cells transfected with empty vector on the right side. Tumor size was monitored every 3–4 days by measuring two perpendicular diameters and the height using a caliper. Mice were killed according to the animal ethical policy of the University of Liège when the apparent size of the tumor exceeded 1,500–2,500 mm^3. Tumors were weighed and then fixed in buffered 3% paraformaldehyde solution for routine histology or embedded in optimal cutting temperature compound (Tissue TeK, Miles Laboratories, Naperville, Ill) and frozen for cryostat sectioning. Cryostat sections (5 µm thick) were fixed first in acetone at −20°C and then in methanol at 4°C before incubation with rat monoclonal antibody against mouse platelet endothelial cell adhesion molecule (PECAM) (Pharmingen). Slides were then incubated with rabbit anti-rat antibody coupled with biotin (E468, Dako) followed by incubation with streptavidin/HRP complex (PO397, Dako). Slides were finally counterstained with hematoxylin and mounted with Eukitt medium for microscope observation.

Results

Recombinant ADAMTS-2 was produced and purified from medium conditioned by HEK 293-EBNA cells transfected with an ADAMTS-2 expression vector. A control sample was produced using HEK 293-EBNA cells transfected with an empty vector and submitted to a purification process identical to that used for recombinant ADAMTS-2. Both preparations were used in parallel in the following experiments.

Effect of ADAMTS-2 on cell proliferation

Recombinant ADAMTS-2 added at increasing concentrations (0.8–5 µg/ml, corresponding to 7–44 nM) significantly reduced the ^{3}H-thymidine uptake by HUVEC after 2 days of contact as compared to the cells treated with the control sample taken as 100% (Fig. 1a, black bars). A similar inhibition of the proliferation was also observed when using HMVEC in the same conditions (Fig. 1a, dark grey bars). No significant effect was found for fibroblasts (Fig. 1a, clear grey bars). The anti-angiogenic effect of ADAMTS-2 was as effective when endothelial cell proliferation was stimulated by VEGF and/or FGF-2 (not shown).

ADAMTS-2 alters endothelial cells morphology and cytoskeleton

After 3 h of seeding on gelatin coat, the three types of endothelial cells (HUVEC, HVMEC, and HMEC) had already well spread (not shown) and their morphology did not change during an additional 16 h incubation in control medium (Fig. 1Ba, b, c). In the presence of ADAMTS-2, subtle changes in endothelial cell morphology were already observed after 15–20 min and accentuated with time (Fig. 1Bd, e, f). Many cells appeared more refringent, retracted and rounded, and clustered into aggregates with many cell protruding processes resembling filipodia and podosomes. Similar results were obtained for bovine aortic endothelial cells (BAEC) (not shown) or for HUVEC and HMEC seeded on gelatin or fibronectin (Fig. S1) or on collagen (not shown). In contrast, ADAMTS-2 did not alter the morphology of human skin fibroblasts (HSF) or smooth-muscle cells (HSMC) (Fig. 1B, compare g, h to i, j).

In order to better visualize the dynamics of the process, time-lapse video microscopy was performed (available as

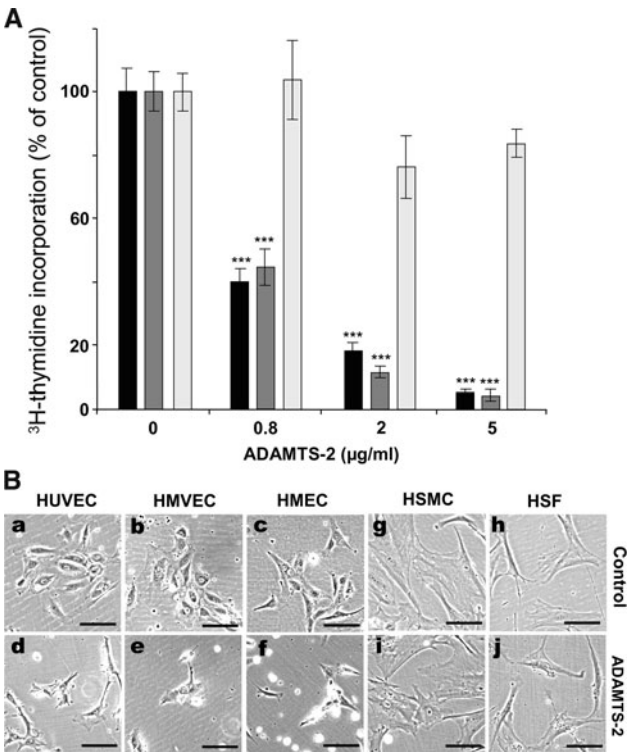

Fig. 1 Recombinant ADAMTS-2 inhibits endothelial cells proliferation and alters their morphology. **a** The proliferation rate of HUVEC (*black bars*), HMVEC (*dark grey bars*), or human skin fibroblasts (*light grey bars*) was measured by ^{3}H-thymidine incorporation in cultures ($n = 6$) supplemented with 0.5% FBS and increasing concentrations (0.8–5 μg/ml) of ADAMTS-2, or of the same volume of the control preparation (0 μg/ml). The results are expressed in percentage of incorporation as compared to the respective controls. The results are representative of three separate experiments for HMVEC and fibroblasts and ten separate experiments for HUVEC. (***$p < 0.001$). **B** Cells were seeded on gelatin coat for 3 h in EBM supplemented with 0.5% FBS and cultured for 16 h in control medium (**a**, **b**, **c**, **g**, **h**) or in the presence of ADAMTS-2 at 5 μg/ml (**d**, **e**, **f**, **i**, **j**). *Bar* 100 μm

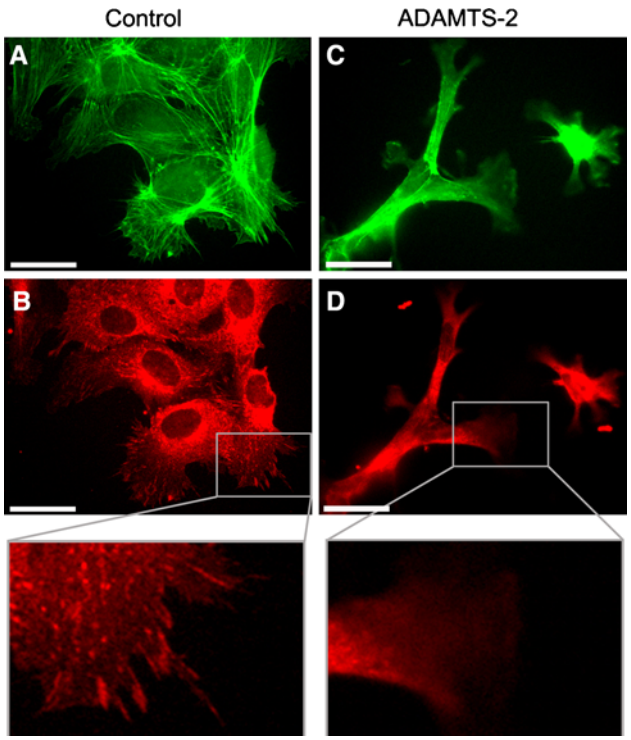

Fig. 2 ADAMTS-2 causes disassembly of actin stress fibers and focal adhesions in HUVEC. HUVEC were seeded on fibronectin coat for 3 h in serum-free EBM and cultured for 16 h in control medium (**a**, **b**) or in medium supplemented with ADAMTS-2 at 5 μg/ml (**c**, **d**). Cells were fixed, permeabilized with 0.1% Triton X-100, and stained to visualize actin stress fibers (FITC-Phalloidin; **a**, **c**) and focal adhesions (anti-vinculin mAb and TRITC-conjugated secondary antibody; **b**, **d**). Focal adhesion appears as small red spots at the extention of actin stress fibers while the diffuse red staining around the nucleus corresponds to cytoplasmic vinculin. *Bar* 25 μm

supplemental material). In control conditions, cells remained well-spread, actively formed membrane ruffles and did not migrate at long distance. In the presence of ADAMTS-2, endothelial cells progressively lost their adherence to the substrate, migrated farther and faster, established cell–cell contacts, assembled into clusters and finally died after 1 day. The same experiment performed with fibroblasts did not show any significant morphological or dynamic changes (not shown).

The organization of the cytoskeleton of HUVEC cultured on fibronectin was visualized by staining fibrillar actin (Fig. 2a) and focal adhesions (Fig. 2b). In control conditions, HUVEC displayed actin stress fibers anchored into focal adhesions as seen in the merged pictures (Fig. 2S). Treatment by ADAMTS-2 for 16 h (Fig. 2c, d) resulted in a disruption of the network of actin stress fibers and dissolution of many focal adhesions, leaving streaks of cortical actin along the protruding processes. Similar results were obtained with HUVEC cultured on gelatin in the presence of ADAMTS-2 (not shown).

ADAMTS-2 induces apoptosis in HUVEC

HUVEC were stained with annexin V-FITC and propidium iodide (PI) and analyzed by FACS in order to evaluate the induction of apoptosis by ADAMTS-2 in the various culture conditions. Due to their limited lifespan in vitro and their high sensitivity towards culture conditions, especially in reduced serum concentration, some apoptotic HUVEC were detected in control conditions (Fig. 3a). Staurosporine, used as positive control, strongly increased apoptosis already after 4 h (Fig. 3b, c, grey bars). In the presence of ADAMTS-2, apoptosis tended to raise already after 4 h and was strongly increased after 20 h as compared to the respective control conditions (Fig. 3b, c, black bars), confirming the time lapse videomicroscopy data (supplemental material).

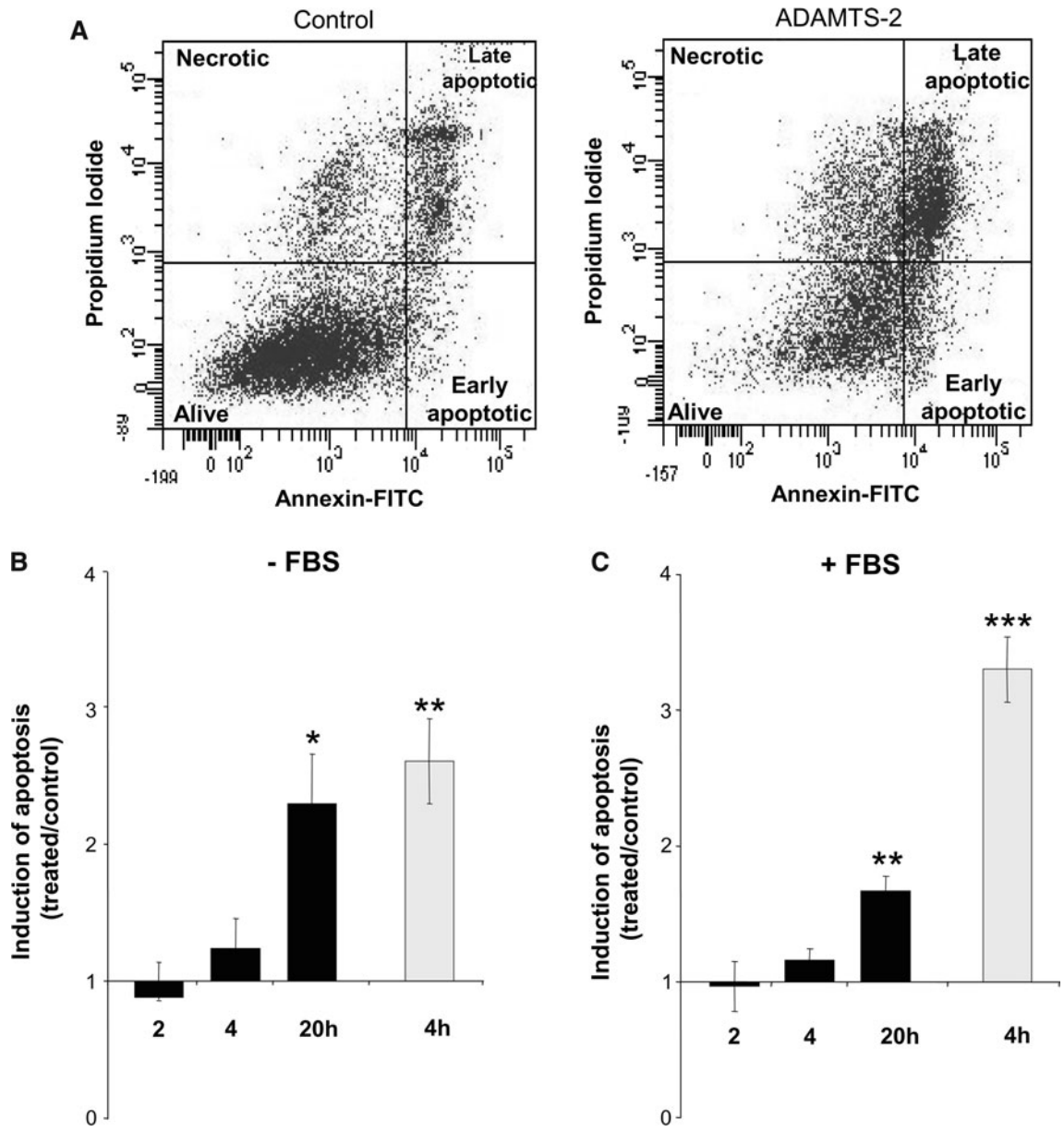

Fig. 3 ADAMTS-2 induces endothelial cell apoptosis. Three hours after seeding without or with 0.5% FBS, culture medium was supplemented with control preparation, ADAMTS-2 (5 μg/ml) or staurosporine (1 μg/ml) as a positive pro-apoptotic control. Cells were then collected after increasing times in culture, stained with annexin V-FITC and PI, and analyzed by FACS. **a** An example of cell distribution is provided (20 h of incubation without FBS in control conditions or in the presence of ADAMTS-2). Total number of cells stained by annexin V-FITC only (early apoptotic) and double stained by annexin V-FITC and PI (late apoptotic) was used to monitor induction of apoptosis by ADAMTS-2 in a time-course experiment in the absence (**b**) or in the presence of (**c**) FBS. The results are expressed as the ratio between the apoptosis induced by ADAMTS-2 (*black bars*) or Staurosporine (*grey bars*) and their respective control (treated/control). **b** $n = 3$; **c** $n = 4$; $^{***}p < 0.001$; $^{**}p < 0.01$; $^{*}p < 0.05$ according to the one-way ANOVA statistical test

ADAMTS-2 destabilizes the capillary-like structures formed in vitro by HUVEC

Confluent monolayers of HUVEC cultured on a thin collagen gel displayed a cobblestone-like morphology (not shown and [29]). Upon addition of a covering collagen gel, cells migrated and formed, within 16 h, capillary-like structures. Addition of ADAMTS-2 only mildly affected the initial steps of this process (Fig. 4, compare e to a, c). This is in agreement with morphology data showing that addition of ADAMTS-2 does not affect cell migration and cell–cell interactions. However,

while the capillary-like structures remained stable for at least 4–5 days in the cultures either containing medium supplemented with FBS alone (Fig. 4Ab, b′) or further supplemented with the control preparation (Fig. 4Ad, d′), the organization of the tube-like structures in the cultures supplemented with ADAMTS-2 was strongly altered after 36 h (Fig. 4Af, f′), with short segments of disassembled vessels and many isolated cells being observed. The quantification of the mean length and number of branchings of the capillary-like structures in the various culture conditions (Fig. 4b, c) further confirmed visual observation.

ADAMTS-2 inhibits vessels formation in embryoid bodies

The properties of ADAMTS-2 were further evaluated in vitro on the differentiation of ES cells into vascular structures in EB induced by VEGF. The vessels were visualized by detection of CD31, in whole-mount

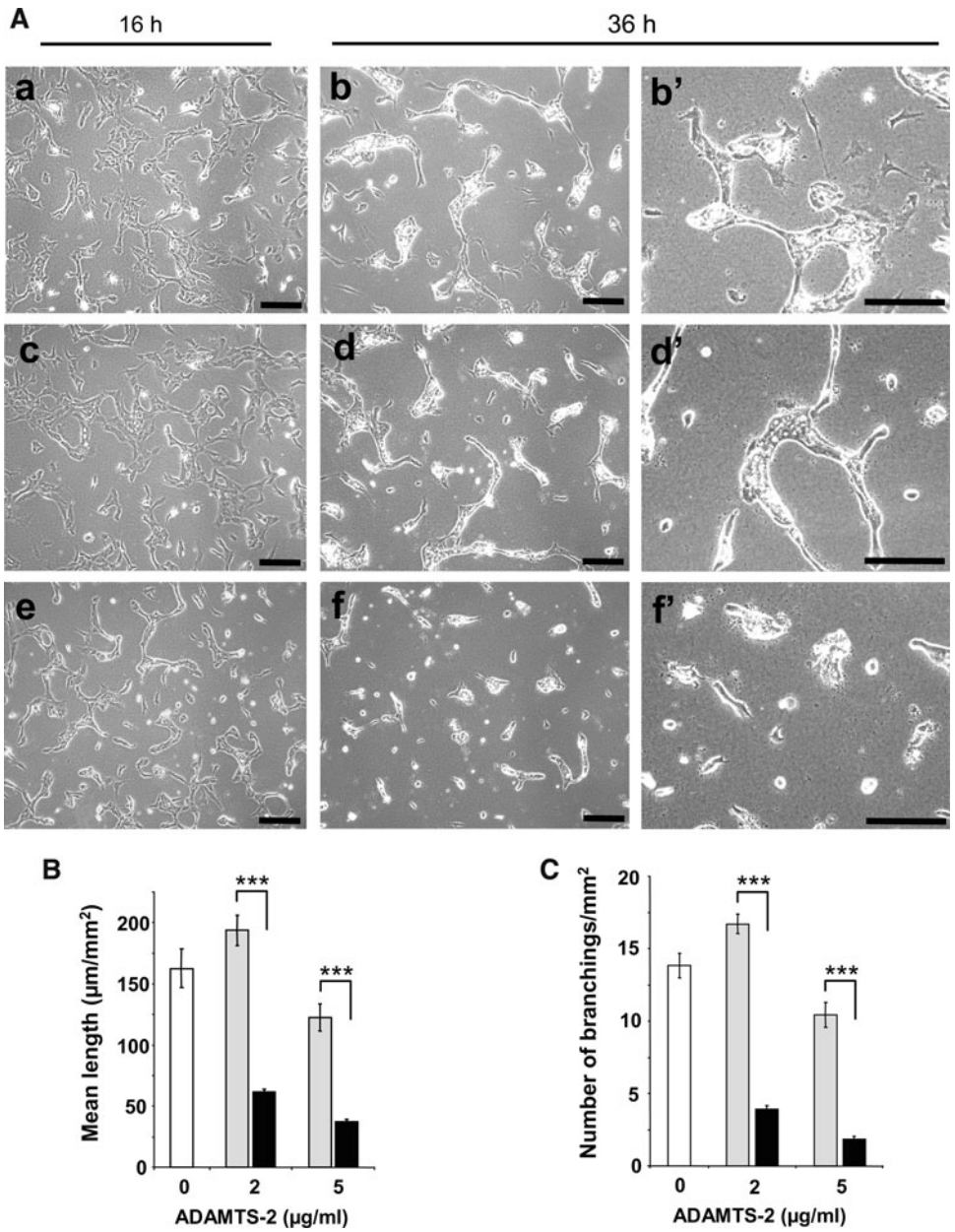

Fig. 4 Effect of ADAMTS-2 on capillary-like structures formed by HUVEC. **A** HUVEC were cultured between two collagen gels in medium containing 10% FBS alone (**a**, **b**), or supplemented with the control preparation (**c**, **d**) or with ADAMTS-2 at 5 µg/ml (**e**, **f**). Pictures were taken after 16 h (**a**, **c**, **e**) or 36 h (**b**, **d**, **f**). *Bars* 100 µm. Mean length of all visible structures (**B**) and number of branching of the capillary-like structures (**C**) were calculated ($n = 30$ pictures) for cultures in medium alone (*open bars*) or supplemented with ADAMTS-2 at 2 or 5 µg/ml (*black bars*) or with the same volume of control sample (*grey bars*). The results are representative of at least three separate experiments (***$p < 0.001$)

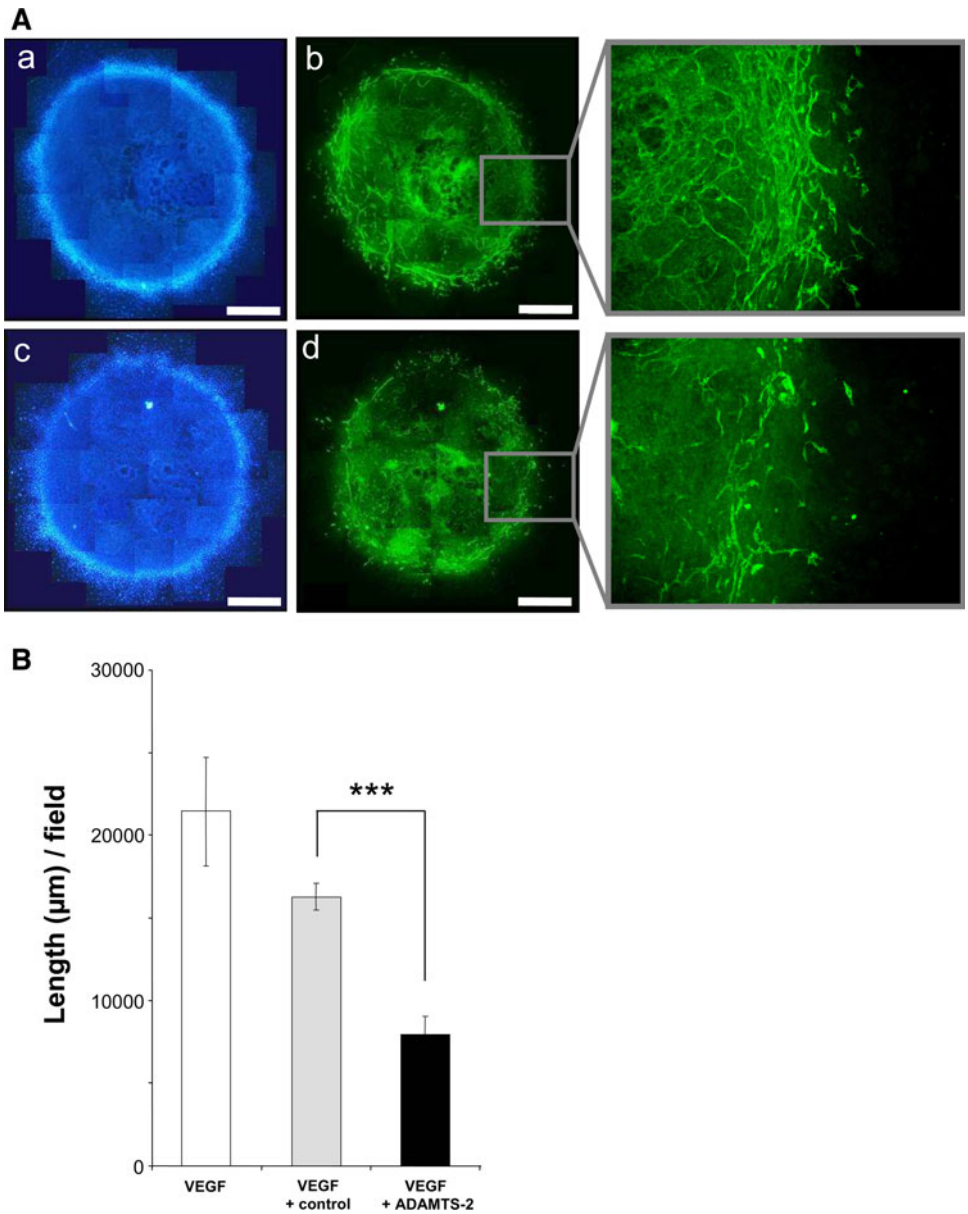

Fig. 5 ADAMTS-2 inhibits the formation of vascular structures in embryoid bodies. **A** Embryoid bodies were formed by culturing ES cells in medium containing VEGF alone (not shown) or further supplemented with the control preparation (**a**, **b**) or with ADAMTS-2 at 0.2 µg/ml (**c**, **d**). Nuclei were stained with DAPI (**a**, **c**) and forming vessels with an anti-CD31 antibody (**b**, **d**). Vessels formed by differentiated endothelial cells appear as elongated and branched green structures. *Bar* 1 mm. **B** Mean length of vessels in EB cultured in medium containing VEGF alone (*open bars*, $n = 3$), or supplemented with control sample (*light grey bars*, $n = 20$), or with ADAMTS-2 at 0.2 µg/ml (*black bars*, $n = 18$) were calculated ($^{***}p < 0.001$)

immunofluorescence microscopy, as a peripheral ring of elongated and branched tubular structures (Fig. 5A). As compared to controls, addition of ADAMTS-2 resulted in a significant reduction of the vessel density (Fig. 5b) without modifying the overall growth of EB as illustrated by DAPI staining of the nuclei (Fig. 5Aa, c). Furthermore, beating heart in EB was not altered by ADAMTS-2 (not shown) as additional evidence that the differentiation and function of other cell types were not impaired.

ADAMTS-2 binds to endothelial cells surface

Live endothelial cells in monolayer cultures were incubated with ADAMTS-2 or the control preparation at 8°C in order to prevent internalization. After fixation and labeling of the non-permeabilized cells with an anti-ADAMTS-2 monoclonal antibody, an intense and punctated staining of endothelial cell surface was observed in cultures supplemented with ADAMTS-2 (Fig. 6, compare a and b). Fibroblasts were also positive (Fig. 6c). In the presence of heparin, the labeling was strongly reduced but not completely abolished (Fig. 6d). Similar effects were observed when cells were pre-treated with sodium chlorate in order to prevent sulfation process (Fig. 6e). This inhibition was completely reversed by adding sodium sulfate together with chlorate to restore sulfation (Fig. 6f). These results suggested the involvement of binding motifs containing heparan sulfate. Similarly, a heparinase III pretreatment strongly reduced, but did not completely abolish, ADAMTS-2 binding at the cell surface (Fig. 6g), while

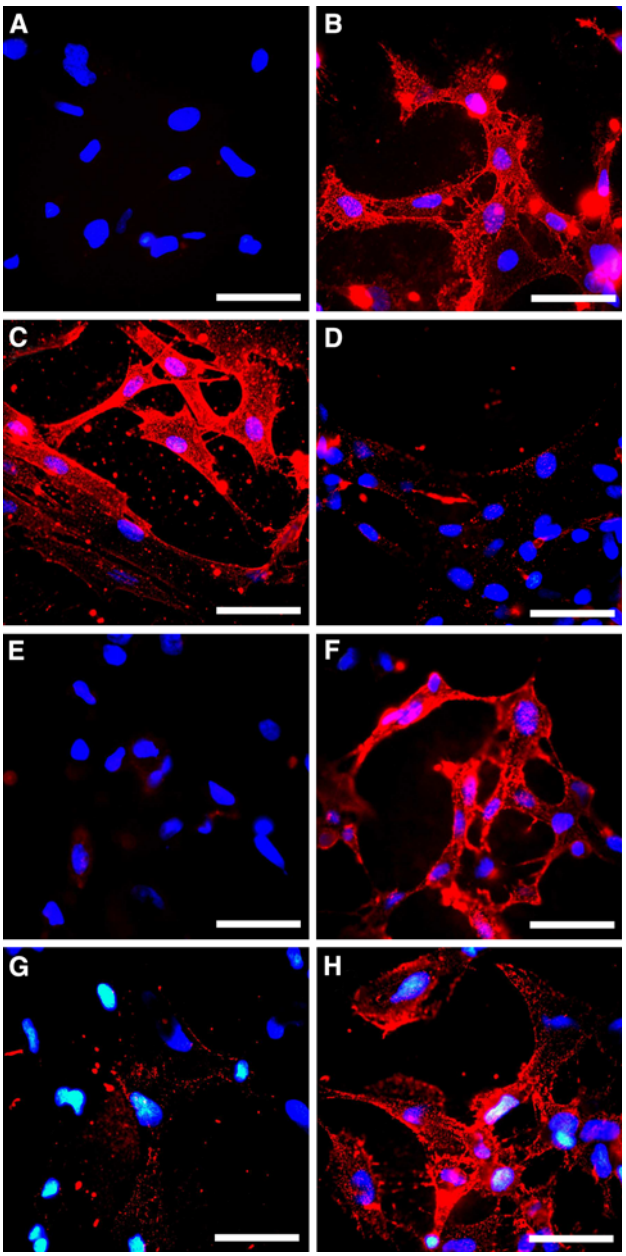

Fig. 6 Binding of ADAMTS-2 at the cell surface. HMEC (**a**, **b**, **d–h**) and fibroblasts (**c**) were incubated for 6 h at 8°C in serum-free medium supplemented with control preparation (**a**) or ADAMTS-2 at 2 μg/ml (**b–h**) in the absence (**a–c**, **e–h**) or presence of 10 μg/ml heparin (**d**) and then immunostained for the presence of ADAMTS-2 immobilized at the cell surface. For a second set of experiments, HMEC were first pretreated for 16 h with 20 mM sodium chlorate alone (**e**) or with sodium chlorate in the presence of 10 mM sodium sulfate (**f**) or for 4 h with 6 mU/ml heparinase III (**g**) or 0.1 U/ml chondroitinase (**h**). After pre-treatment, medium was changed and cells were cultured for 6 h at 8°C in the presence of ADAMTS-2 before staining as described above. *Bar* 50 μm

digestion with chondroitinase had no effect (Fig. 6h). In another set of experiments, cells initially preincubated with ADAMTS-2 at 8°C were brought to 37°C and immunostained at increasing time after re-warming. In these conditions, an active internalization process was visualized already after 15 min and was almost complete after 2 h (not shown).

Although the participation of heparan sulphate proteoglycans (HSPG) in ADAMTS-2 immobilization at the cell surface was firmly established, heparinase III pretreatment did not significantly modify the effect of ADAMTS-2 on endothelial cell morphology and proliferation (not shown), suggesting the existence of a signaling cell surface receptor. For its identification, extracts of endothelial cell membranes were submitted to column chromatography on either immobilized ADAMTS-2 as a bait or non-coupled resin as control. Besides a few unspecific proteins eluting from both columns, nucleolin was identified by peptide mass fingerprinting in two fractions specifically eluted from the ADAMTS-2 coupled resin. These data were further confirmed by Western blotting, which identified four different processed forms of nucleolin (Fig. S3).

Co-localization studies were performed in order to evaluate the interaction between ADAMTS-2 and nucleolin in a cellular context. Non-permeabilized endothelial cells were successively pretreated with heparinase III, incubated at 8°C with ADAMTS-2 and fixed before double immunostaining of ADAMTS-2 and nucleolin (Fig. 7). The pattern of surface nucleolin was punctated and spread over the entire cell surface. The nuclei remained negative, confirming the absence of cell permeabilization. Staining of ADAMTS-2 also revealed a punctated pattern. These positive spots were less numerous than spots positive for nucleolin but always colocalized with nucleolin positive structures as illustrated by the yellow to orange colors on the merge pictures. Most of these double-positive spots were localized at the cell edge.

ADAMTS-2 intracellular signaling

The phosphorylation status of various signaling proteins was assessed after addition of ADAMTS-2 to serum-starved spread HUVEC. A slight repression of FAK phosphorylation was induced by addition of ADAMTS-2, as compared to control (Fig. 8a). A progressive reduction of the total amount of FAK with time was also observed in some experiments but was not further investigated since it was not regulated by the presence of ADAMTS-2. Myosin light chain, an operational protein of the actin stress-fibers, was investigated. A decreased level of phosphorylation was already apparent after 10 min of incubation with ADAMTS-2 and persisted for at least 2 h (Fig. 8b). By using Y27632, a Rho kinase (ROCK) inhibitor, the level of phosphorylated MLC was also strongly reduced (not shown). However, this reduction did not result in alteration of cell morphology, and did not prevent or increase the effect of ADAMTS-2. The level of phosphorylated Erk1/2

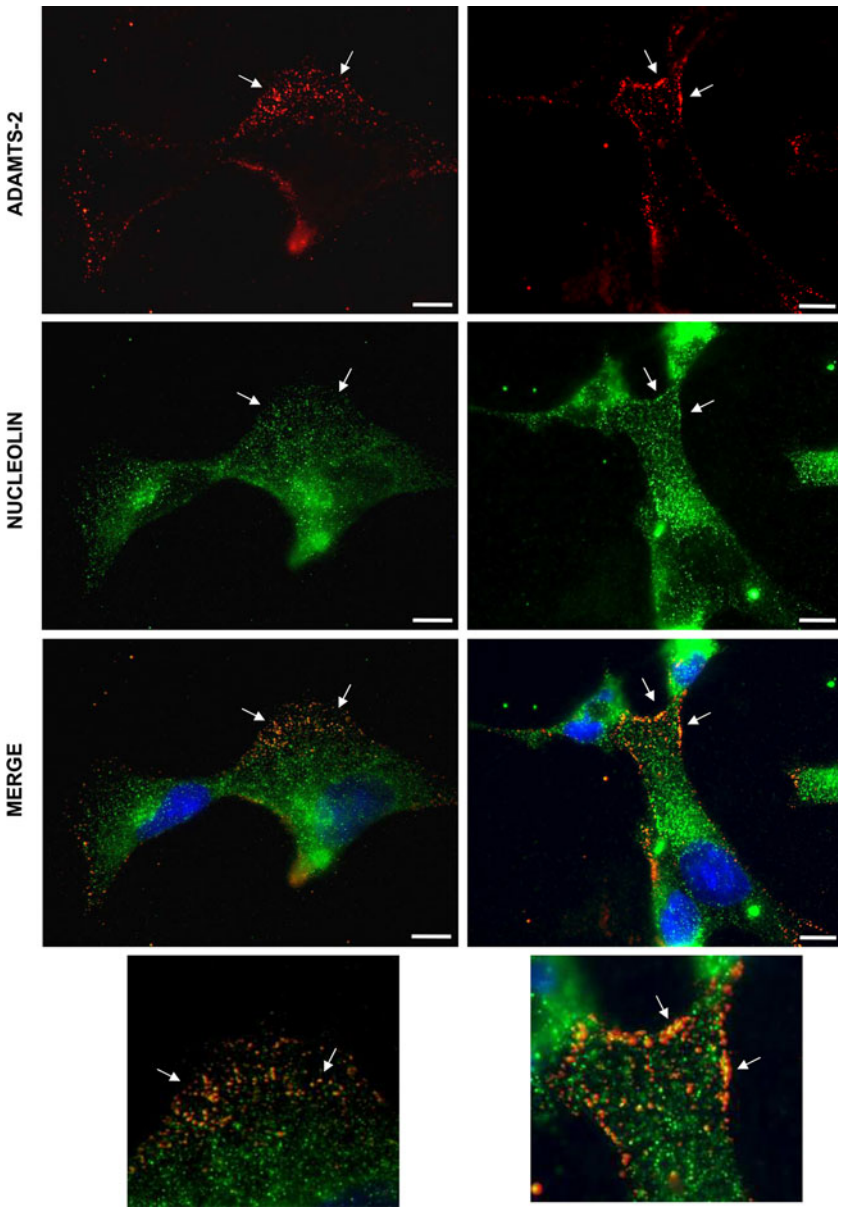

Fig. 7 ADAMTS-2 and nucleolin co-localization at the cell-surface HMEC were pretreated for 4 h with 6 mU/ml heparinase III, incubated for 6 h at 8°C in serum-free medium supplemented with ADAMTS-2 at 0.5 μg/ml, and stained to visualize ADAMTS-2 (*red*) and nucleolin (*green*) at the cell surface. A merged picture of the two stainings shows co-localization of the two proteins (*arrows*). *Bar* 10 μm

decreased with time in control conditions while a much faster reduction of phosphorylation was induced by ADAMTS-2 in HUVEC (Fig. 8c) whereas it was not modified, or even slightly increased, in fibroblasts (Fig. 8d). Phosphorylation of two other signaling proteins, PAK and p38, was not modified by ADAMTS-2 (not shown).

Targeted deletion of ADAMTS-2 in mice results in an increased angiogenic response to ocular LASER injury

Wild-type (WT) and ADAMTS-2 deficient (ADAMTS-$2^{-/-}$) mice were used in a model of choroidal neovascularization following LASER burn injury. Fourteen days after LASER impact, the delay for maximal neovascularization [31], the mice were perfused with dextran-fluorescein and the vascular density was evaluated using confocal microscopy and digital image capture. Neovascularization was observed only at the sites initially injured by the LASER and was significantly and reproducibly higher in ADAMTS-$2^{-/-}$ as compared to WT mice (Fig. S4). Evaluation, by quantitative RT-PCR, of the level of various mRNA coding for proteins involved in healing and angiogenesis as listed in Table S1 (supplemental material) was also performed. No difference was observed between WT and ADAMTS-$2^{-/-}$ for any mRNA and at any time point after LASER burn (not shown).

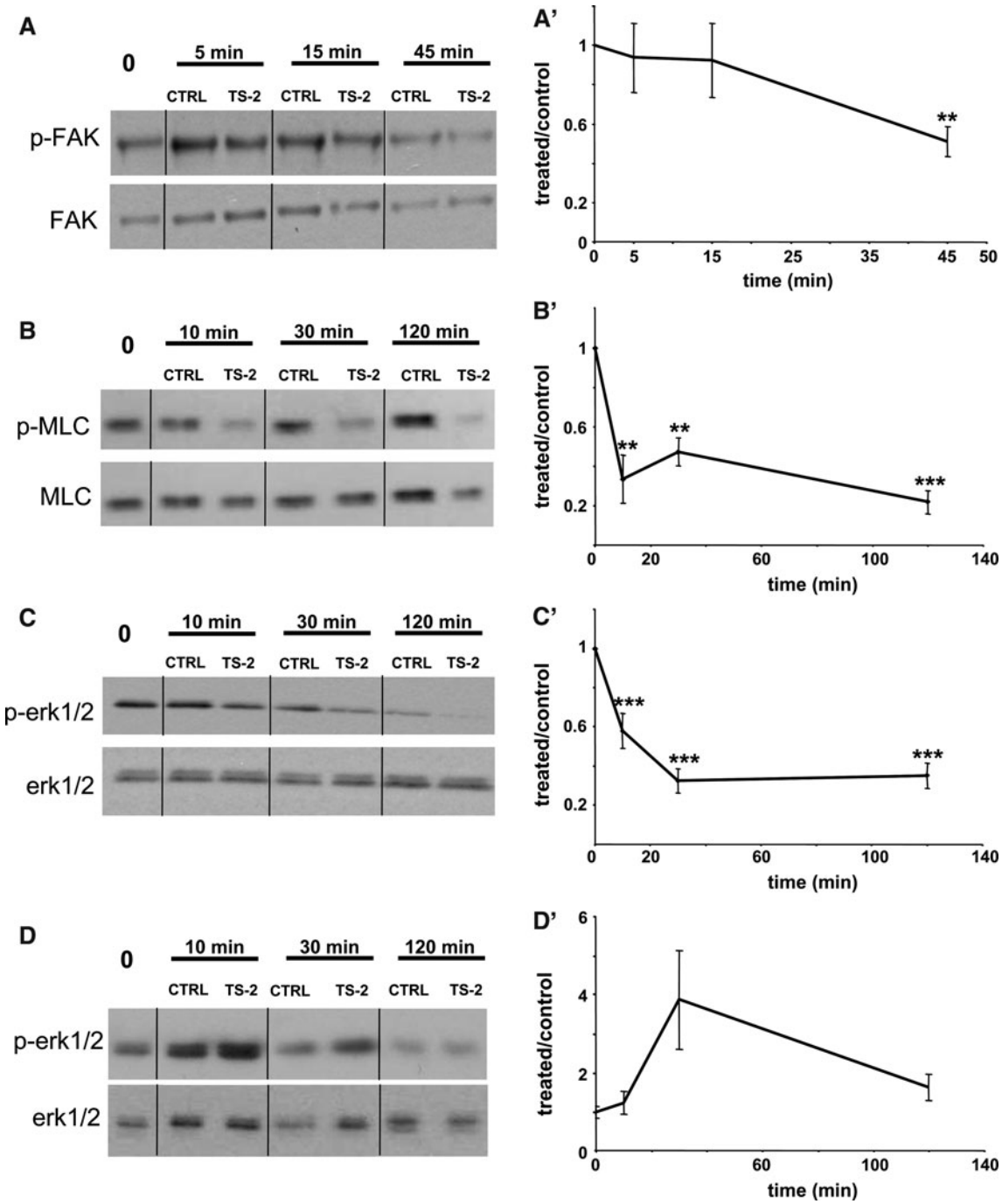

Fig. 8 Effect of ADAMTS-2 on the phosphorylation of Erk1/2, MLC and FAK. HUVEC (**a**, **b**, **c**) or fibroblasts (**d**) were seeded in serum-free medium and allowed to spread for 3 h at 37°C. ADAMTS-2 (TS-2) and control preparation (CTRL) were then added for various times. Cell lysates were analyzed by Western blotting using antibodies for phosphorylated FAK (p-FAK) and total FAK (**a**), phosphorylated MLC (p-MLC) and total MLC (**b**) and phosphorylated Erk1/2 (p-Erk1/2) and total Erk1/2 (**c**, **d**). Scanning density of the bands obtained in at least three independent experiments was used to calculate the relative level of p-FAK versus total FAK ($n = 6$) (**a**′), p-MLC versus total MLC ($n = 3$) (**b**′) and p-Erk1/2 versus total Erk1/2 ($n = 8$) (**c**′, **d**′) in the various cultures conditions (***$p < 0.001$; **$p < 0.01$)

ADAMTS-2 inhibits tumor growth

HEK 293-EBNA cells stably transfected with the control vector or expressing ADAMTS-2 were mixed with Matrigel and subcutaneously injected in the flanks of six nude mice, control cells in one side, and ADAMTS-2 expressing cells in the contralateral side. The six plugs containing control cells generated growing tumors

(Fig. 9a). By contrast, tumoral development was not observed in the ADAMTS-2 expressing cells, only one out of the six ADAMTS-2 plugs starting to slightly grow at day 30. After killing, dissected tumors were weighed, clearly demonstrating a dramatic difference in the mean tumoral mass (Fig. 9b). While control tumors appeared reddish with a well-developed peritumoral vascular network (Fig. 9c), ADAMTS-2 expressing tumors were whiter and little vascularized. A Western-blot analysis failed to reveal significant accumulation of ADAMTS-2 at the time of the animal killing, suggesting that most of the HEK 293-EBNA cells expressing ADAMTS-2 either died or stopped to produce ADAMTS-2. This was confirmed by immunohistochemistry analysis showing that only a few cells at the periphery of tumors was still producing ADAMTS-2 (not shown). A second independent experiment ($n = 4$) performed in similar conditions gave identical results, further demonstrating the efficiency and the reproducibility of the inhibition (Fig. 12a). Histological examination revealed the presence of large aggregates of HEK 293-EBNA cells in control tumors (Fig. 10a), containing both capillaries and larger vessels (Fig. 10b). In the small tumors formed by cells expressing ADAMTS-2, necrotic areas and collapsed vessels were noted (Fig. 10a, b).

The catalytic activity of ADAMTS-2 is dispensable for antiangiogenic activity

Three additional constructs coding for catalytically inactive ADAMTS-2 or for ADAMTS-2 lacking either the central or the C-terminal domains were created and used for stable transfection of HEK 293-EBNA cells. The proliferation rate of these cell lines in vitro was similar and close to that of the control cells or cells expressing the wild-type enzyme (Fig. 12e). These cells were also used for the production of recombinant enzymes. Out of these three ADAMTS-2 mutants, only the catalytically inactive form could be purified using the protocol developed for the wild-type enzyme. The electrophoretic pattern of these two recombinant forms was strongly different (Fig. 11a) since the wild-type form was essentially found as a fully processed molecule from which both the prodomain and the PNP domain are cleaved while the catalytic mutant still retained the PNP domain as previously described [19]. Their relative effects were compared in various in vitro models. The catalytic mutant was able to modify both the morphology (Fig. 11b) and the proliferation rate (Fig. 11c) of endothelial cells although less drastically than observed for the wild-type enzyme. Both types of enzymes bound also with a similar efficiency to the surface of endothelial cells (Fig. 11d).

The cell lines expressing the wild-type and the three mutant forms of ADAMTS-2 were evaluated for their ability to generate tumors (Fig. 12a–d). While the injection of control cells resulted in the formation of rapidly growing tumors, none of the three mutant cell lines induce significant tumoral growth. This shows that the three mutated forms of ADAMTS-2, including the catalytically inactive form, were as efficient as the wild-type enzyme for preventing tumor growth.

Discussion

Angiogenesis plays a critical role in cancer progression and metastasis [32]. Tumor growth and dissemination have been shown to be dependent on neovascularization, explaining why inhibition of tumoral angiogenesis by selectively inhibiting growth, survival, and migration of endothelial cells is still perceived today as an attractive tool for controlling cancer progression [3, 33, 34]. The potential anti-angiogenic properties of ADAMTS-2 were hypothesized on the basis of similarities between sequences and domains involved in the inhibitory activity of thrombospondin 1 and 2 and ADAMTS-1 and -8. Antiproliferative properties of recombinant ADAMTS-2 was first investigated on endothelial cell cultures in monolayer. ADAMTS-2 reproducibly inhibited the proliferation of microvascular and umbilical vein endothelial cells, with a maximal repression observed between 1 and 5 μg/ml. These concentrations ($\sim$5–40 nM) are in the same range as those reported for thrombospondin 2 [35] and ADAMTS-1 and -8 [14]. At similar concentrations, the proliferation of human fibroblasts and smooth-muscle cells was not altered, demonstrating the specificity towards endothelial cells. As opposed to ADAMTS-1 [13], the anti-proliferative effect of ADAMTS-2 on endothelial cells does not seem to result from interactions with a growth factor or interference with a growth factor pathway as the relative repression exerted by ADAMTS-2 was similar in the absence or presence of VEGF and/or FGF-2.

Morphological changes induced by ADAMTS-2 were evaluated using cells cultured on various extracellular matrices in the absence of any mitogenic stimulus. The alterations, observed within the first hour of contact and worsening with time, consisted of a progressive detachment and retraction of the cellular body with the persistence of thin extensions resembling filipodia. Actin cytoskeleton and focal adhesions were also rapidly and profoundly disorganized. The observed changes were similar in endothelial cells spread onto various extracellular matrix proteins, suggesting that either most of the integrins are targeted by ADAMTS-2 or that they are not involved in the process. Analysis of the entire process by videomicroscopy clearly confirmed the progressive loss of contact between endothelial cells and the matrix, further

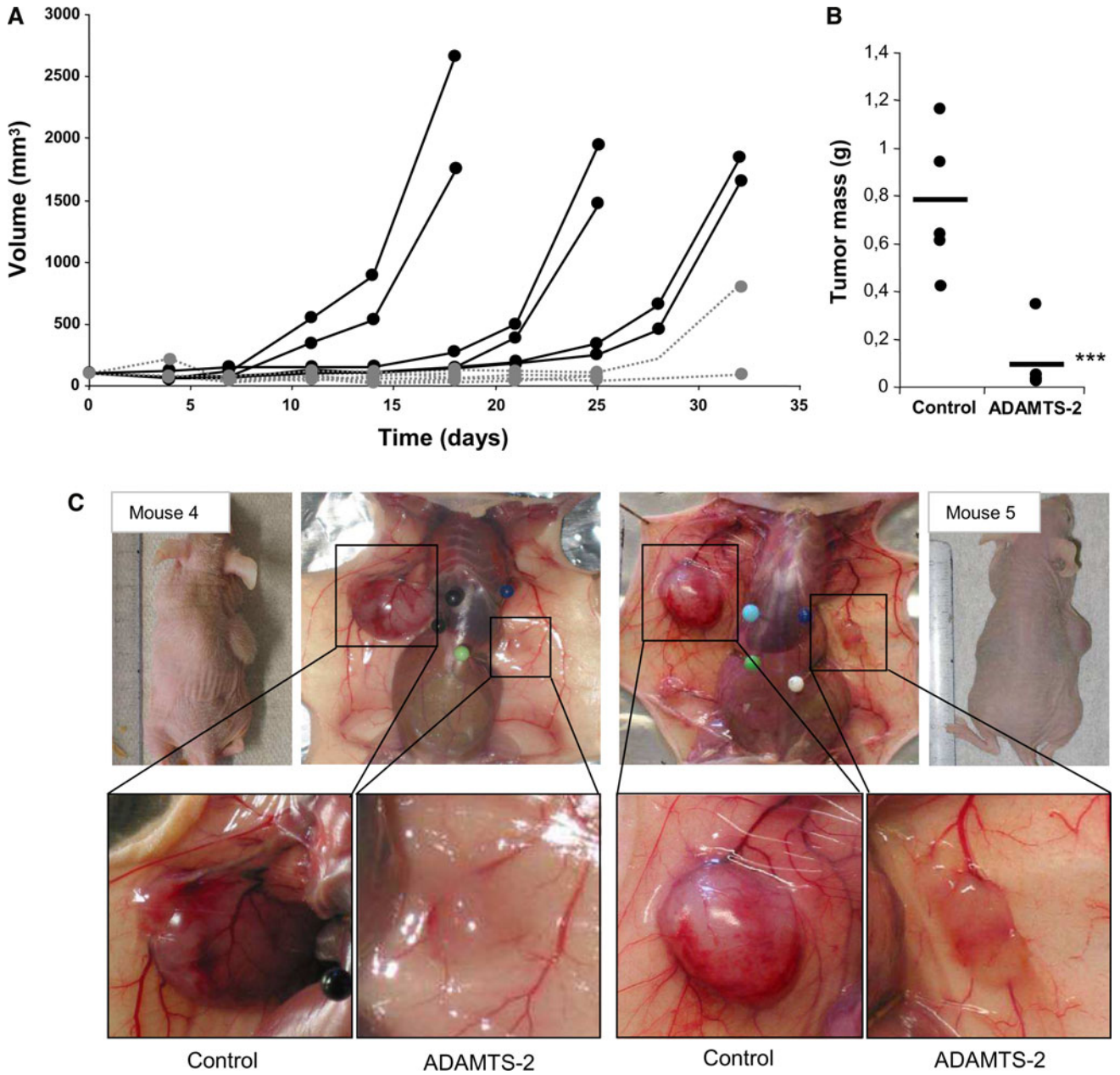

Fig. 9 ADAMTS-2 inhibits growth of HEK 293-EBNA tumors in nude mice. HEK 293-EBNA cells stably transfected with empty vector or expressing ADAMTS-2 were mixed with Matrigel and subcutaneously injected into each flank of the mice, one with control cells (control) and the other with ADAMTS-2 (TS-2) expressing cells ($n = 6$). **a** Growth of plugs containing control cells (*plain black lines*) or ADAMTS-2 expressing cells (*dotted grey lines*) was evaluated by measuring the tumor's volume every 3–4 days. Mice were killed when the apparent volume of one of the bilateral tumors reached 1,500 mm^3. **b** Mean values of tumor mass for control cells and ADAMTS-2-expressing cells (***$p < 0.001$). **c** Aspect of the tumors in toto and before dissection in two representative mice

resulting in rapid random cell movements, formation of cell clusters, and ultimately cell death. The presence of numerous blebbing cells and the results of FACS analysis were both indicative of a pro-apoptotic activity of ADAMTS-2, most probably by anoikis.

The rapidity of the effect of ADAMTS-2 strongly suggested the existence of early alterations of intracellular regulatory pathways. Addition of ADAMTS-2 to endothelial cells indeed resulted in a reduced phosphorylation of MLC within 10 min, a feature that would explain the fast and pronounced disorganization of the actin cytoskeleton and rounding of the cells. The decreased phosphorylation of FAK observed at later time points in ADAMTS-2 treated cells might also result from such cytoskeleton disruption. In astrocytes, the RhoA/ROCK1/MLC pathway regulates the process of actin

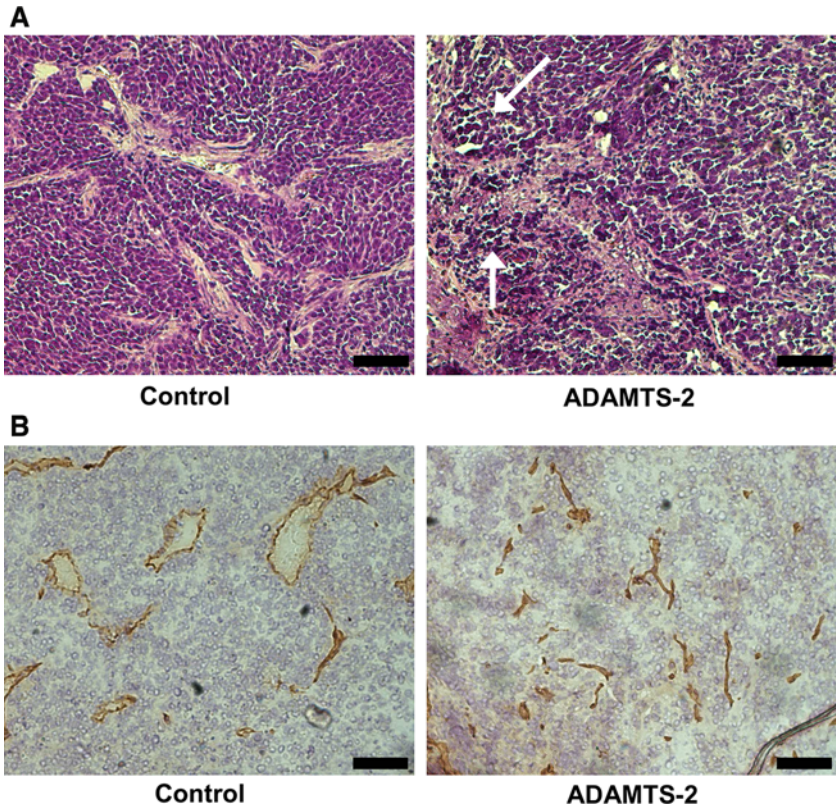

Fig. 10 Immunohistological examination of control and ADAMTS-2-expressing tumors. **a** Paraffin sections of tumors formed by control or by ADAMTS-2-expressing cells were stained with hematoxylin and eosin stain (H&E). Necrotic cells were visible only in ADAMTS-2 tumors (*arrows*). **b** Cryostat sections of tumors were stained by an anti-CD31 antibody for visualizing blood vessels (*in brown*). *Bar* 100 μm

reorganization, cell retraction and rounding, and anoikis [36]. In our cells, inhibition of ROCK by Y27632 strongly decreased the level of phosphorylated MLC, demonstrating the efficiency of this inhibitor, but did not mimic (neither prevent) the effect of ADAMTS-2. This indicated that this specific pathway was not essential in our model. Similarly, Rac1-, Cdc42-, and p38-mediated pathways did not seem to be involved since the phosphorylation of PAK and p38 was not modified. By contrast, binding of ADAMTS-2 to the endothelial cell surface rapidly repressed the phosphorylation of Erk1/2, an ubiquitous intracellular mediator implicated in various pathways regulating a large array of cell functions. A similar effect on Erk1/2 activity was recently observed for ADAMTS-12 using Madin-Darby Canine Kidney (MDCK) cells [37]. This inhibition was already evident after 10 min, before any visible morphological alterations, suggesting that modification of the Erk1/2 signaling is perhaps one of the causes (not consequences) of the disorganization of actin cytoskeleton. This is also in agreement with our data regarding fibroblasts. Although these cells bind a large amount of ADAMTS-2 at their surface, they are not affected in terms of morphology and survival, which correlates with a different pattern of response in terms of Erk1/2 phosphorylation.

The rapid and strong response of endothelial cells to ADAMTS-2 suggested a direct interaction between cells and the enzyme. Such interaction was evidenced after incubation of endothelial cells with recombinant ADAMTS-2 and visualization of cell surface-bound enzyme. Interestingly, fibroblasts were also strongly labeled, although they were not affected by ADAMTS-2 in terms of survival, proliferation, and morphology. ADAMTS-2 binding to the endothelial cell surface is heparin-, heparinase III-, and chlorate-sensitive, suggesting that it involves, directly or indirectly, a heparan sulfate proteoglycan (HSPG). However, although efficient in terms of preventing ADAMTS-2 binding, heparinase III treatment did not significantly prevent the pro-apoptotic effect of ADAMTS-2 on endothelial cells. Although it could not be completely ruled out that it is related to an incomplete cleavage of HS-side chains, a more likely explanation would be that HSPG are not necessary to mediate the signaling induced by ADAMTS-2. There are indeed many examples showing that HSPG can bind growth factors (FGF-2, VEGF, …), potentiating their biological activity by increasing their local concentration and availability near their specific receptors, but are not strictly required for the transmission of the growth factor signal [38, 39]. Affinity chromatography using ADAMTS-2 as a bait and co-localization studies identified nucleolin as a potential membrane receptor for ADAMTS-2. Nucleolin was initially described as a nucleolar protein participating in the transcriptional control of ribosomal RNA genes, in ribosomes maturation and assembly, and in the

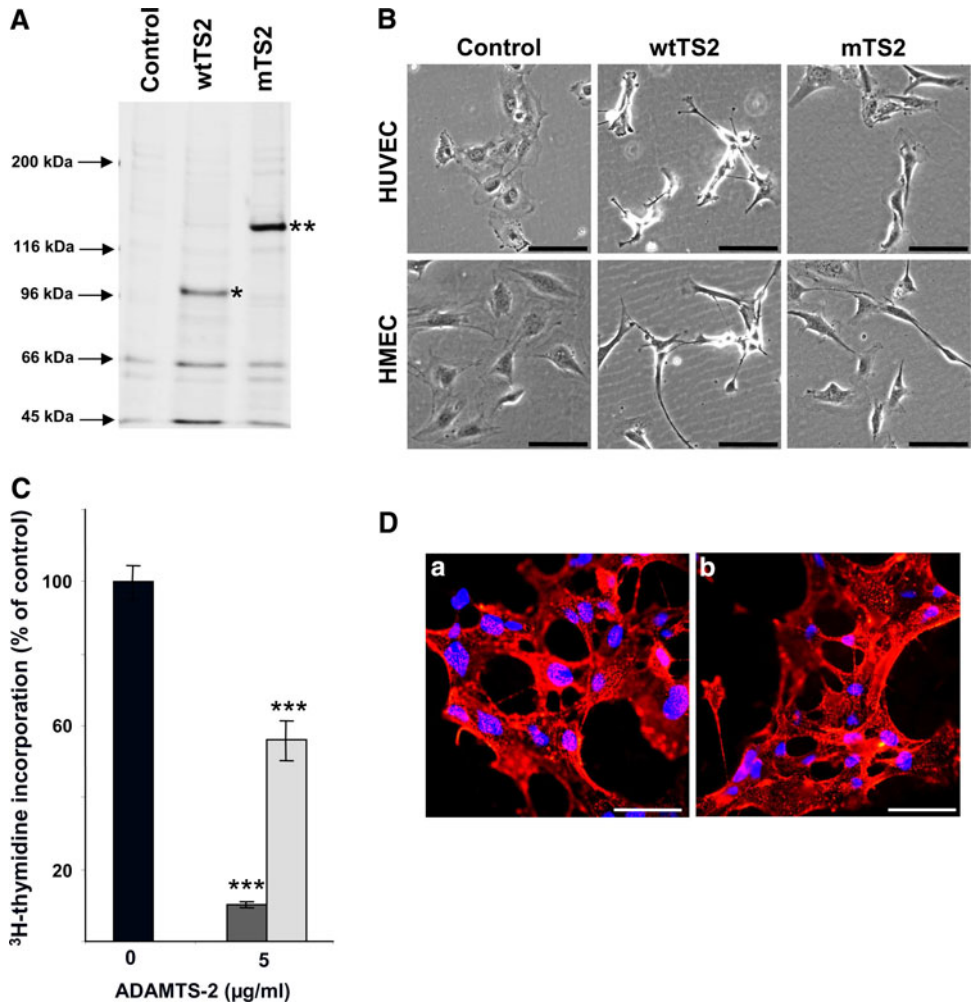

Fig. 11 The catalytic activity of ADAMTS-2 is dispensable for antiangiogenic activity. **a** Sypro Ruby staining of purified control preparation (control), wild-type ADAMTS-2 (wtTS2) or catalytically inactive ADAMTS-2 (mTS-2). *Asterisks* indicate the most abundant form of ADAMTS-2 (* for wild-type ADAMTS-2 and ** for catalytically inactive ADAMTS-2). **b** HUVEC or HMEC were seeded on gelatin coats for 3 h in serum-free EBM and cultured for 16 h in medium supplemented with the control preparation (control), the wild-type ADAMTS-2 (wtTS-2) or catalytically inactive ADAMTS-2 (mTS-2), both at 5 µg/ml. *Bar* 100 µm. **c** The proliferation rate of HUVEC was measured by ^{3}H-thymidine uptake in cultures ($n = 6$) in the presence of wtTS2 (*dark grey bar*), of mTS2 (*light grey bar*) both at 5 µg/ml, or of the same amount of control preparation (0 µg/ml, *black bar*). The results are representative of three separate experiments (***$p < 0.001$). **d** HMEC were incubated for 6 h at 8°C in serum-free medium supplemented with wild-type ADAMTS-2 (**a**) or catalytically inactive ADAMTS-2 (**b**) both at 2 µg/ml and immunostained for the presence of ADAMTS-2 immobilized at the cell surface. *Bar* 50 µm

nucleocytoplasmic transport of ribosomal components [40, 41]. It has also been shown that nucleolin can translocate to the plasma membrane in some specific cell types such as endothelial cells and many transformed cells [42]. When present at the cell surface, it has been shown that nucleolin can interact with Erb B receptors or serves as a receptor for L-selectin, midkine and, most interestingly, endostatin [43], a potent anti-angiogenic fragment of collagen XVIII. The implication of nucleolin in the control of angiogenesis was strengthened by recent publications showing that an antibody targeting the acidic domain of nucleolin caused apoptosis of cultured endothelial cells and was anti-angiogenic in vitro and in vivo [44]. A direct interaction between this acidic domain and ADAMTS-2 would not be surprising considering that ADAMTS-2 has affinity for the negatively charged heparin and HSPG and that the heparin-binding domain of endostatin is required for its efficient binding on the acidic domain of nucleolin. Moreover, a specific antagonist of cell-surface nucleolin reduces the phosphorylation of Erk1/2 within a few minutes and suppresses tumor growth and angiogenesis [45], two features also observed here for ADAMTS-2. The hypothesis that nucleolin is a receptor mediating the proapoptotic effect of ADAMTS-2 may seemed challenged by the observation that HEK 293-EBNA cells are not affected by ADAMTS-2 although they express nucleolin at

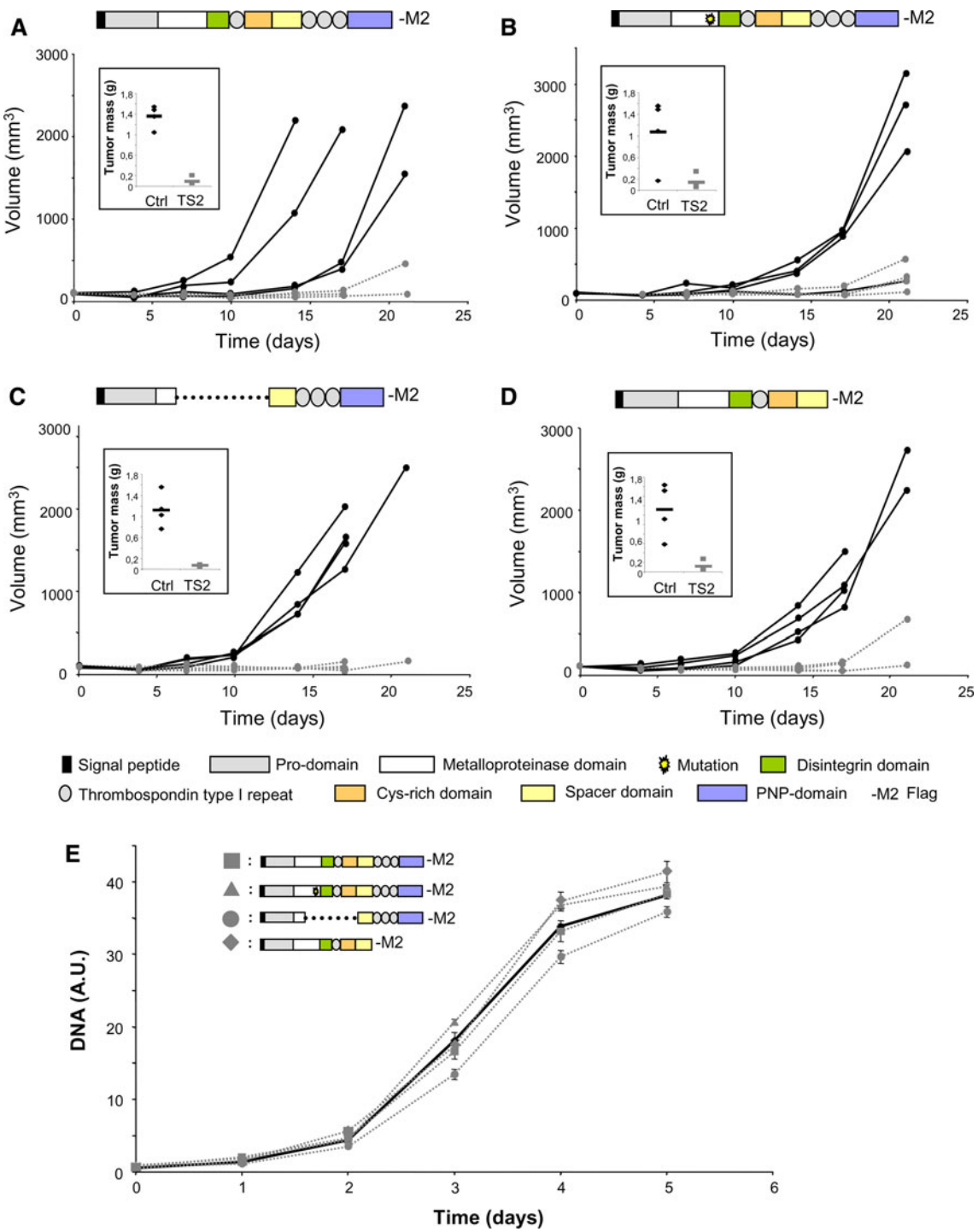

Fig. 12 Effect of different recombinant forms of ADAMTS-2 on tumor growth. The experimental procedure was as detailed in Fig. 9 ($n = 4$). A schematic domains organization of the four different recombinant ADAMTS-2 expressed by cells forming the tumors is provided at the top of each corresponding graphics. Tumor volume was measured every 3–4 days. Control tumors are represented by *bold plain black lines* while tumors formed by the different forms of ADAMTS-2 are illustrated by *dotted grey lines* (**a** wild-type ADAMTS-2; **b** mutated catalytically inactive ADAMTS-2; **c** ADAMTS-2 lacking the central domains including the metalloproteinase domain; **d** ADAMTS-2 lacking the C-terminal domains). Insets in **a**–**d** illustrate the mean tumor mass after dissection. **e** The proliferation rate of control HEK-293 EBNA cells (*bold dark line*) or of HEK-293 EBNA cells expressing the different forms of ADAMTS-2 (*dotted grey lines*) was evaluated by DNA quantification

their surface (not shown). Similar data have been obtained with endostatin, which induces apoptosis in endothelial cells and some transformed cells while other cell types, although expressing nucleolin, are not altered [43]. Cell-specific intracellular pathways or the requirement of specific membrane co-receptors may explain this apparent discrepancy. Due to its vital importance for many cellular processes, we consider that repression of nucleolin by RNAi would not be appropriate for evaluating its implication as a "receptor" mediating apoptosis. Moreover, the amount of cell surface nucleolin may not be directly correlated to its overall abundance. Specific targeting of membrane nucleolin would be more suitable but is currently impossible because of the unavailability of blocking antibodies.

The antiangiogenic properties of ADAMTS-2 were also assessed in vivo. In a choroidal neovascularization model [46], a reproducible and significant increase of neovascularization was observed in ADAMTS-$2^{-/-}$ mice as compared to wild-type animals, supporting an antiangiogenic function for ADAMTS-2 in vivo. In a second model, HEK 293-EBNA cells were grafted subcutaneously to induce formation of tumors in nude mice [47]. The parental cells formed rapidly growing tumors characterized by the development of a dense network of functional blood vessels. When cells expressing wild-type ADAMTS-2 were used, tumor growth was drastically reduced, the small cell plugs were whiter and many necrotic areas were detected. Since control cells and cells expressing ADAMTS-2 grow at a similar rate, all these observations are most probably related to the absence of an efficient blood supply since only small and collapsed vessels are present in these tumors, again illustrating the anti-angiogenic properties of ADAMTS-2.

The same models were used to identify the specific domain(s) of ADAMTS-2 that is responsible for its anti-angiogenic effects. Three different types of mutated ADAMTS-2 were produced. The catalytically inactive ADAMTS-2, resulting from a point mutation in the metalloproteinase domain, could be purified with the same efficiency as the wild-type enzyme. However, its molecular size is different since a functional catalytic pocket is required for the autocatalytic processing of PNP terminal domain [19]. As an additional difference, it was found that this incompletely processed form tends to form aggregates and to precipitate when purified and concentrated in physiological saline conditions (D. Hulmes, unpublished data). The two other recombinant enzymes, lacking either the central or the C-terminal domains, could not be sufficiently purified using procedures developed for the wild-type ADAMTS-2, most probably due to the absence of specific sequences and glycosylation required for affinity chromatography. Therefore only the recombinant ADAMTS-2 lacking metalloproteinase activity was evaluated in vitro for its effects on angiogenesis. It binds on endothelial cells and alters their morphology and proliferation rate, although to a lesser extent than the wild-type enzyme. It clearly demonstrates that the effect of ADAMTS-2 on endothelial cells does not directly involve its catalytic activity. It also shows that the persistence of the PNP domain has functional consequences in in vitro model of angiogenesis possibly by modifying availability and/or exposure of specific domains at the surface of the molecule or by reducing the solubility and therefore the specific concentration of ADAMTS-2. As the model of tumor growth does not require a purification process, it was used to evaluate the effect of the three mutant forms of ADAMTS-2 (Fig. 12). The catalytically inactive ADAMTS-2 efficiently prevented tumor growth, in agreement with the in vitro data. The two other mutated variants lacking specific domain were also active in restricting tumor growth. This would indicate that a common domain is responsible for the effect. The pro-domain is certainly not implicated since it is cleaved during secretion and is not present in purified enzyme used in vitro [19]. This would indicate that the short aminoterminal extremity of the metalloproteinase domain and/or the 132 amino acid-long spacer domain, which are common in all these constructs, are possibly involved. The spacer domain of ADAMTS-4 or ADAMTS-5 has been shown to modulate the proteolytic activity of the enzyme [48] but a structural function unrelated to the enzymatic activity has never been described so far. As an alternative hypothesis, antiangiogenic activity could be operated by two different TSR1 domains: the first, which is the only one present in the ADAMTS-2 lacking the C-terminal domain, and any of the three TSR1 that are still conserved in the ADAMTS-2 deprived of its central domain. The initial observations of the antiangiogenic potential of TSR1 domains were made during the study of thrombospondins 1 and 2 [8]. Various other TSR1 domains from different types of proteins, including ADAMTS-4, -16 and -18, have been previously tested [49]. Some of them significantly reduced (10–50%) endothelial cell proliferation but only at much higher concentration (500 nM–20 μM) as compared to the active concentration of ADAMTS-2 used here (2 μg/ml; around 16 nM). It has also been shown that the first (but not the second) TSR1 of ADAMTS-5 inhibited proliferation and increased apoptosis of endothelial cells at concentration ranging from 100 to 1,000 nM. Concerning ADAMTS-1 its antiangiogenic effect largely results from its specific interactions with VEGF165 [13] or depends on its catalytic activity [16], two mechanisms that are not implicated for ADAMTS-2. These data show that these closely related enzymes can affect angiogenesis with different efficiency and through different pathways. They also illustrate the

significance and the complexity of their functions and, therefore, demonstrate the need of an extensive characterization of both their active domain(s) and their specific receptor(s).

Acknowledgments This work was supported by grants from the Belgian Fonds de la Recherche Scientifique Médicale (Grant nos. 3.4362.03 and 3.4387.05), the Belgian Fonds National de la Recherche Scientifique, the "Foundation against Cancer", the "Fondation Léon Fredericq" (University of Liège), the "Centre Anticancéreux près l'Université de Liège" and the "Région Wallonne" (NeoAngio, grant no. 616476). We thank the "Proteomic" (M.-A. Meuwis) and "Imaging and Flow cytometry" (Sandra Ormenese) platforms of GIGA-R (University of Liège) and Dr. Prockop (Texas A&M Health Science Center, USA) for the kind gift of ADAMTS-2 $^{-/-}$ mice.

References

1. Bix G, Iozzo RV (2005) Matrix revolutions: "tails" of basement-membrane components with angiostatic functions. Trends Cell Biol 15:52–60
2. Sottile J (2004) Regulation of angiogenesis by extracellular matrix. Biochim Biophys Acta 1654:13–22
3. Folkman J (1972) Anti-angiogenesis: new concept for therapy of solid tumors. Ann Surg 175:409–416
4. Armstrong LC, Bornstein P (2003) Thrombospondins 1 and 2 function as inhibitors of angiogenesis. Matrix Biol 22:63–71
5. Lee NV, Sato M, Annis DS, Loo JA, Wu L, Mosher DF, Iruela-Arispe ML (2006) ADAMTS1 mediates the release of antiangiogenic polypeptides from TSP1 and 2. EMBO J 25:5270–5283
6. Adams JC (2001) Thrombospondins: multifunctional regulators of cell interactions. Annu Rev Cell Dev Biol 17:25–51
7. Febbraio M, Hajjar DP, Silverstein RL (2001) CD36: a class B scavenger receptor involved in angiogenesis, atherosclerosis, inflammation, and lipid metabolism. J Clin Invest 108:785–791
8. Tolsma SS, Volpert OV, Good DJ, Frazier WA, Polverini PJ, Bouck N (1993) Peptides derived from two separate domains of the matrix protein thrombospondin-1 have anti-angiogenic activity. J Cell Biol 122:497–511
9. Grant MA, Kalluri R (2005) Structural basis for the functions of endogenous angiogenesis inhibitors. Cold Spring Harb Symp Quant Biol 70:399–410
10. O'Reilly MS, Holmgren L, Shing Y, Chen C, Rosenthal RA, Moses M, Lane WS, Cao Y, Sage EH, Folkman J (1994) Angiostatin: a novel angiogenesis inhibitor that mediates the suppression of metastases by a Lewis lung carcinoma. Cell 79:315–328
11. Wahl ML, Kenan DJ, Gonzalez-Gronow M, Pizzo SV (2005) Angiostatin's molecular mechanism: aspects of specificity and regulation elucidated. J Cell Biochem 96:242–261
12. Heljasvaara R, Nyberg P, Luostarinen J, Parikka M, Heikkila P, Rehn M, Sorsa T, Salo T, Pihlajaniemi T (2005) Generation of biologically active endostatin fragments from human collagen XVIII by distinct matrix metalloproteases. Exp Cell Res 307:292–304
13. Luque A, Carpizo DR, Iruela-Arispe ML (2003) ADAMTS1/METH1 inhibits endothelial cell proliferation by direct binding and sequestration of VEGF165. J Biol Chem 278:23656–23665
14. Vazquez F, Hastings G, Ortega MA, Lane TF, Oikemus S, Lombardo M, Iruela-Arispe ML (1999) METH-1, a human ortholog of ADAMTS-1, and METH-2 are members of a new family of proteins with angio-inhibitory activity. J Biol Chem 274:23349–23357
15. Iruela-Arispe ML, Luque A, Lee N (2004) Thrombospondin modules and angiogenesis. Int J Biochem Cell Biol 36:1070–1078
16. Iruela-Arispe ML, Carpizo D, Luque A (2003) ADAMTS1: a matrix metalloprotease with angioinhibitory properties. Ann NY Acad Sci 995:183–190
17. Colige A, Beschin A, Samyn B, Goebels Y, Van Beeumen J, Nusgens BV, Lapiere CM (1995) Characterization and partial amino acid sequencing of a 107-kDa procollagen I N-proteinase purified by affinity chromatography on immobilized type XIV collagen. J Biol Chem 270:16724–16730
18. Colige A, Li SW, Sieron AL, Nusgens BV, Prockop DJ, Lapiere CM (1997) cDNA cloning and expression of bovine procollagen I N-proteinase: a new member of the superfamily of zinc-metalloproteinases with binding sites for cells and other matrix components. Proc Natl Acad Sci USA 94:2374–2379
19. Colige A, Ruggiero F, Vandenberghe I, Dubail J, Kesteloot F, Van Beeumen J, Beschin A, Brys L, Lapiere CM, Nusgens B (2005) Domains and maturation processes that regulate the activity of ADAMTS-2, a metalloproteinase cleaving the aminopropeptide of fibrillar procollagens types I–III and V. J Biol Chem 280:34397–34408
20. Colige A, Sieron AL, Li SW, Schwarze U, Petty E, Wertelecki W, Wilcox W, Krakow D, Cohn DH, Reardon W, Byers PH, Lapiere CM, Prockop DJ, Nusgens BV (1999) Human Ehlers-Danlos syndrome type VII C and bovine dermatosparaxis are caused by mutations in the procollagen I N-proteinase gene. Am J Hum Genet 65:308–317
21. Wang WM, Lee S, Steiglitz BM, Scott IC, Lebares CC, Allen ML, Brenner MC, Takahara K, Greenspan DS (2003) Transforming growth factor-beta induces secretion of activated ADAMTS-2. A procollagen III N-proteinase. J Biol Chem 278:19549–19557
22. Colige A, Nuytinck L, Hausser I, van Essen AJ, Thiry M, Herens C, Ades LC, Malfait F, Paepe AD, Franck P, Wolff G, Oosterwijk JC, Smitt JH, Lapiere CM, Nusgens BV (2004) Novel types of mutation responsible for the dermatosparactic type of Ehlers-Danlos syndrome (Type VIIC) and common polymorphisms in the ADAMTS2 gene. J Invest Dermatol 123:656–663
23. Li SW, Arita M, Fertala A, Bao Y, Kopen GC, Langsjo TK, Hyttinen MM, Helminen HJ, Prockop DJ (2001) Transgenic mice with inactive alleles for procollagen N-proteinase (ADAMTS-2) develop fragile skin and male sterility. Biochem J 355:271–278
24. Jaffe EA, Nachman RL, Becker CG, Minick CR (1973) Culture of human endothelial cells derived from umbilical veins. Identification by morphologic and immunologic criteria. J Clin Invest 52:2745–2756
25. Ades EW, Candal FJ, Swerlick RA, George VG, Summers S, Bosse DC, Lawley TJ (1992) HMEC-1: establishment of an immortalized human microvascular endothelial cell line. J Invest Dermatol 99:683–690
26. Colige AC, Lambert CA, Nusgens BV, Lapiere CM (1992) Effect of cell-cell and cell-matrix interactions on the response of fibroblasts to epidermal growth factor in vitro. Expression of collagen type I, collagenase, stromelysin and tissue inhibitor of metalloproteinases. Biochem J 285(Pt 1):215–221
27. Millette E, Rauch BH, Defawe O, Kenagy RD, Daum G, Clowes AW (2005) Platelet-derived growth factor-BB-induced human smooth muscle cell proliferation depends on basic FGF release and FGFR-1 activation. Circ Res 96:172–179
28. Labarca C, Paigen K (1980) A simple, rapid, and sensitive DNA assay procedure. Anal Biochem 102:344–352

29. Deroanne CF, Colige AC, Nusgens BV, Lapiere CM (1996) Modulation of expression and assembly of vinculin during in vitro fibrillar collagen-induced angiogenesis and its reversal. Exp Cell Res 224:215–223
30. Deroanne CF, Bonjean K, Servotte S, Devy L, Colige A, Clausse N, Blacher S, Verdin E, Foidart JM, Nusgens BV, Castronovo V (2002) Histone deacetylases inhibitors as anti-angiogenic agents altering vascular endothelial growth factor signaling. Oncogene 21:427–436
31. Tobe T, Ortega S, Luna JD, Ozaki H, Okamoto N, Derevjanik NL, Vinores SA, Basilico C, Campochiaro PA (1998) Targeted disruption of the FGF2 gene does not prevent choroidal neovascularization in a murine model. Am J Pathol 153:1641–1646
32. Hanahan D, Weinberg RA (2000) The hallmarks of cancer. Cell 100:57–70
33. Kerbel RS (1991) Inhibition of tumor angiogenesis as a strategy to circumvent acquired resistance to anti-cancer therapeutic agents. Bioessays 13:31–36
34. Kerbel RS (2008) Tumor angiogenesis. N Engl J Med 358:2039–2049
35. Noh YH, Matsuda K, Hong YK, Kunstfeld R, Riccardi L, Koch M, Oura H, Dadras SS, Streit M, Detmar M (2003) An N-terminal 80-kDa recombinant fragment of human thrombospondin-2 inhibits vascular endothelial growth factor induced endothelial cell migration in vitro and tumor growth and angiogenesis in vivo. J Invest Dermatol 121:1536–1543
36. Minambres R, Guasch RM, Perez-Arago A, Guerri C (2006) The RhoA/ROCK-I/MLC pathway is involved in the ethanol-induced apoptosis by anoikis in astrocytes. J Cell Sci 119:271–282
37. Llamazares M, Obaya AJ, Moncada-Pazos A, Heljasvaara R, Espada J, Lopez-Otin C, Cal S (2007) The ADAMTS12 metalloproteinase exhibits anti-tumorigenic properties through modulation of the Ras-dependent ERK signalling pathway. J Cell Sci 120:3544–3552
38. Grunewald FS, Prota AE, Giese A, Ballmer-Hofer K (2010) Structure-function analysis of VEGF receptor activation and the role of coreceptors in angiogenic signaling. Biochim Biophys Acta 1804:567–580
39. Kinsella MG, Irvin C, Reidy MA, Wight TN (2004) Removal of heparan sulfate by heparinase treatment inhibits FGF-2-dependent smooth muscle cell proliferation in injured rat carotid arteries. Atherosclerosis 175:51–57
40. Di Segni A, Farin K, Pinkas-Kramarski R (2008) Identification of nucleolin as new ErbB receptors-interacting protein. PLoS One 3:e2310
41. Srivastava M, Pollard HB (1999) Molecular dissection of nucleolin's role in growth and cell proliferation: new insights. FASEB J 13:1911–1922
42. Christian S, Pilch J, Akerman ME, Porkka K, Laakkonen P, Ruoslahti E (2003) Nucleolin expressed at the cell surface is a marker of endothelial cells in angiogenic blood vessels. J Cell Biol 163:871–878
43. Shi H, Huang Y, Zhou H, Song X, Yuan S, Fu Y, Luo Y (2007) Nucleolin is a receptor that mediates antiangiogenic and antitumor activity of endostatin. Blood 110:2899–2906
44. Fogal V, Sugahara KN, Ruoslahti E, Christian S (2009) Cell surface nucleolin antagonist causes endothelial cell apoptosis and normalization of tumor vasculature. Angiogenesis 12:91–100
45. Destouches D, El Khoury D, Hamma-Kourbali Y, Krust B, Albanese P, Katsoris P, Guichard G, Briand JP, Courty J, Hovanessian AG (2008) Suppression of tumor growth and angiogenesis by a specific antagonist of the cell-surface expressed nucleolin. PLoS One 3:e2518
46. Lambert V, Wielockx B, Munaut C, Galopin C, Jost M, Itoh T, Werb Z, Baker A, Libert C, Krell HW, Foidart JM, Noel A, Rakic JM (2003) MMP-2 and MMP-9 synergize in promoting choroidal neovascularization. FASEB J 17:2290–2292
47. Mineur P, Colige AC, Deroanne CF, Dubail J, Kesteloot F, Habraken Y, Noel A, Voo S, Waltenberger J, Lapiere CM, Nusgens BV, Lambert CA (2007) Newly identified biologically active and proteolysis-resistant VEGF-A isoform VEGF111 is induced by genotoxic agents. J Cell Biol 179:1261–1273
48. Fushimi K, Troeberg L, Nakamura H, Lim NH, Nagase H (2008) Functional differences of the catalytic and non-catalytic domains in human ADAMTS-4 and ADAMTS-5 in aggrecanolytic activity. J Biol Chem 283:6706–6716
49. Karagiannis ED, Popel AS (2007) Anti-angiogenic peptides identified in thrombospondin type I domains. Biochem Biophys Res Commun 359:63–69